T-type channel blockade impairs long-term potentiation at the parallel fiber–Purkinje cell synapse and cerebellar learning

Romain Ly[a,b,c,1], Guy Bouvier[a,b,c,1], Martijn Schonewille[d,1], Arnaud Arabo[e,f,g,1], Laure Rondi-Reig[f,g], Clément Léna[a,b,c], Mariano Casado[a,b,c], Chris I. De Zeeuw[d,h,2], and Anne Feltz[a,b,c,2]

[a]Institut de Biologie de l'Ecole Normale Supérieure, IBENS, F-75005 Paris, France; [b]Centre National de la Recherche Scientifique (CNRS), Unité Mixte de Recherche (UMR) 8197, F-75005 Paris, France; [c]École Normale Supérieure, F-75005 Paris, France; [d]Department of Neuroscience, ErasmusMC, 3015 GE, Rotterdam, The Netherlands; [e]Unité de Formation et de Recherche des Sciences et Techniques, Université de Rouen, 76821 Mont Saint Aignan Cedex, France; [f]Université Pierre et Marie Curie Univ Paris 6, F-75005 Paris, France; [g]CNRS, UMR 7102, F-75005 Paris, France; and [h]Netherlands Institute for Neuroscience, 1105 BA, Amsterdam, The Netherlands

Edited by Eve Marder, Brandeis University, Waltham, MA, and approved October 29, 2013 (received for review June 21, 2013)

$Ca_V3.1$ T-type channels are abundant at the cerebellar synapse between parallel fibers and Purkinje cells where they contribute to synaptic depolarization. So far, no specific physiological function has been attributed to these channels neither as charge carriers nor more specifically as Ca^{2+} carriers. Here we analyze their incidence on synaptic plasticity, motor behavior, and cerebellar motor learning, comparing WT animals and mice where T-type channel function has been abolished either by gene deletion or by acute pharmacological blockade. At the cellular level, we show that $Ca_V3.1$ channels are required for long-term potentiation at parallel fiber–Purkinje cell synapses. Moreover, basal simple spike discharge of the Purkinje cell in KO mice is modified. Acute or chronic T-type current blockade results in impaired motor performance in particular when a good body balance is required. Because motor behavior integrates reflexes and past memories of learned behavior, this suggests impaired learning. Indeed, subjecting the KO mice to a vestibulo-ocular reflex phase reversal test reveals impaired cerebellum-dependent motor learning. These data identify a role of low-voltage activated calcium channels in synaptic plasticity and establish a role for $Ca_V3.1$ channels in cerebellar learning.

Neurotransmission at the parallel fiber (PF) and Purkinje cell (PC) synapse plays a pivotal role in cerebellar motor learning probably involving bidirectional changes of its strength (1–3). Unlike in the hippocampus, postsynaptic Ca^{2+} signaling at PF–PC spines may not be dominated by ionotropic glutamatergic receptors, as postsynaptic N-methyl-D-aspartate receptors (NMDARs) are not prominently present at this site and AMPA receptors are predominantly impermeable for calcium ions (4, 5). PCs bear different voltage-dependent Ca channels including P/Q-type (6–8) and T-type channels (9, 10). The spines of PCs contain a high density of $Ca_V3.1$ T-type channels (11), which can be readily activated by typical bursts of PF activity that occur during sensory stimulation (12–14). To date, the function of the PF to PC synapse plays a pivotal role in cerebellar motor learning, probably involving bidirectional changes of its strength (1–3). Unlike in the hippocampus, T-type channels during PF–PC plasticity induction and cerebellar learning has not been explored.

In cerebellar PCs, the elevation of Ca^{2+} in the spine has been suggested to control directly the sign of the changes in synaptic weights (15). Long-term depression (LTD) induction requires conjunctive stimulation of the climbing fibers (CFs) and PFs, which triggers a large supralinear calcium entry mediated by mGluR1, inositol triphosphate (IP3) receptors and voltage-gated calcium channels (16–19). In contrast, long-term potentiation (LTP) develops after PF stimulation only and requires a moderate $[Ca^{2+}]_i$ elevation (15). Here, we evaluated the hypothesis that $Ca_V3.1$ T-type channel activation is essential for LTP and LTP-dependent motor learning.

We first looked at PF–PC plasticity of T-type channel blockade/deletion, and then investigated both in vitro and in vivo the dynamics of PC activity as well as the motor behavior of both wild-type and $Ca_V3.1$ KO mice. Because, in our experiments, motor behavior appears to be impaired in tests requiring a refined body balance, we have analyzed vestibulo-ocular reflex (VOR) adaptation, a learning paradigm more specifically dependent on vestibulo-cerebellar function. We show all three processes to be impaired after T-type channel functional inactivation. We propose that T-type calcium channels contribute to the definition of the learning rules in the cerebellar cortex.

Results

T-Type Channel Blockade Prevents LTP Induction with No Effect on LTD. We have studied the role of T-type calcium channels in the induction of LTP by applying a burst of PF stimuli (five pulses, 200 Hz) every second during 5 min. This protocol increases the excitatory postsynaptic current (EPSC) charge to 203% ± 15% of baseline in wild-type (WT) mice ($n = 8$, $P = 0.008$, Fig. 1 *A* and *B*). Paired-pulse facilitation (PPF) is not significantly altered after LTP induction (1.60 ± 0.10 vs. 1.75 ± 0.15 before and after induction protocol, respectively; $n = 8$, $P = 0.50$; Table S1), consistent with the postsynaptic expression of this form of potentiation

Significance

T-type calcium channels are present in the spines of a number of principal neurons. In absence of specific antagonists, their function has been difficult to elucidate. At the cerebellar synapse between parallel fiber (PF) and Purkinje cell (PC), postsynaptic Ca^{2+} signaling is not the result of ionotropic glutamatergic receptor activation, while T-type $Ca_V3.1$ channels are abundantly expressed in PCs. We show that they are required for long-term potentiation but not for long-term depression at PF–PC synapses. Because plasticity at this site has long been proposed to be important for cerebellar forms of motor learning, we have checked the behavioral incidence of acute or chronic blockade of T-type channels. In this condition, we show impairment of demanding cerebellar motor learning tasks.

Author contributions: R.L., G.B., M.S., A.A., L.R.-R., C.L., M.C., C.I.D.Z., and A.F. designed research; R.L., G.B., M.S., A.A., and A.F. performed research; R.L., G.B., M.S., A.A., L.R.-R., C.L., M.C., C.I.D.Z., and A.F. analyzed data; and R.L., G.B., M.S., A.A., M.C., C.I.D.Z., and A.F. wrote the paper.

The authors declare no conflict of interest.

This article is a PNAS Direct Submission.

Freely available online through the PNAS open access option.

[1]R.L., G.B., M.S., and A.A. contributed equally to this work.

[2]To whom correspondence may be addressed. E-mail: feltz@ens.fr or c.dezeeuw@erasmusmc.nl.

This article contains supporting information online at www.pnas.org/lookup/suppl/doi:10.1073/pnas.1311686110/-/DCSupplemental.

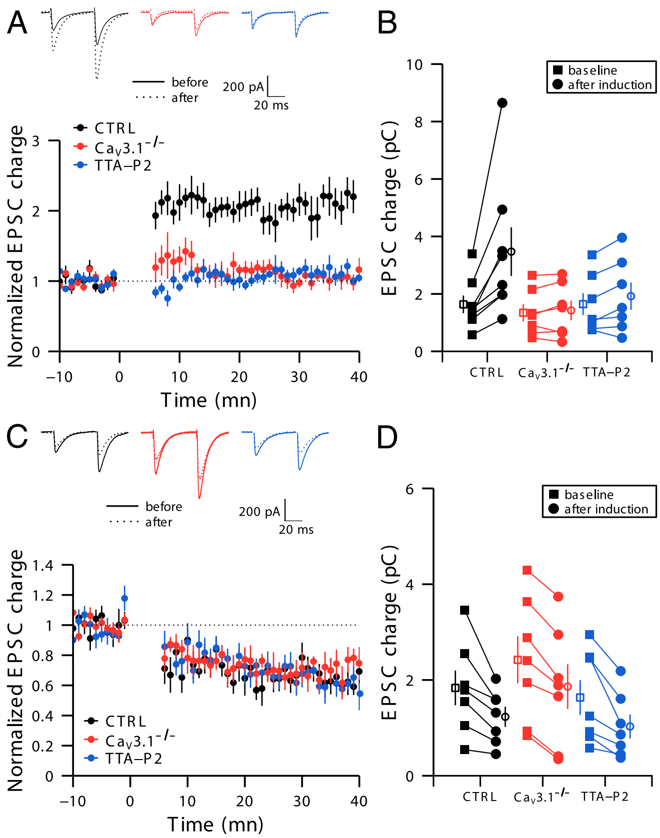

Fig. 1. Activation of T-type calcium channels is necessary to induce PF–PC LTP but not for LTD. (*A* and *B*) T-type calcium channels are required for LTP induction. (*A*, *Upper*) Representative traces from 10 successive sweeps before and 30 min after induction of LTP. (*A*, *Lower*) Time course of normalized EPSC charge in control (black), in the continuous presence of 1 μM TTA-P2 (blue), and in $Ca_V3.1^{-/-}$ mice (red). The LTP induction protocol started at time 0. (*B*) EPSC charge before and 30 min after LTP induction. Filled symbols represent individual cells, whereas empty symbols represent means. Black, red, and blue indicate results from control mice, from $Ca_V3.1^{-/-}$ mice, and in the presence of TTA-P2, respectively, and corresponding n = 8, 7, and 7 individual experiments for the three sets of mice, each run on a different slice. Note that data from some cells are superimposed. (*C* and *D*) T-type calcium channels are not required for LTD induction. (*C*, *Upper*) Representative traces from 10 successive sweeps before and 30 min after induction of LTD. (*C*, *Lower*) Time course of normalized EPSC charge in control (black), 1 μM TTA-P2 (blue), and in $Ca_V3.1^{-/-}$ mice (red). The LTD induction protocol started at time 0. (*D*) EPSC charge before and 30 min after LTD induction. n = 7 individual experiments from different slices for the three sets of conditions.

(15, 20). In contrast, LTP is completely absent in $Ca_V3.1^{-/-}$ mice (101% ± 8%; $n = 7$, $P = 0.52$; Fig. 1 *A* and *B*). Acute inactivation of T-type calcium channels in WT mice by a selective T-type antagonist (1 μM TTA-P2) (21) also prevents LTP induction (113% ± 10% of baseline; $n = 7$, $P = 0.21$; Fig. 1 *A* and *B*). Again, paired-pulse ratio remains unchanged after LTP induction (Table S1).

We next investigated the impact of blocking T-type channels on LTD induction in WT mice. Doublets of PF stimuli (two pulses, 200 Hz) followed by a 100 ms burst of CF activation (four pulses, 400 Hz) every second during 5 min reliably induced LTD in controls (EPSC decreased to 70% ± 4% of baseline; $n = 7$, $P = 0.015$), in the presence of 1 μM TTA-P2 (63% ± 5% of baseline; $n = 7$, $P = 0.015$), and in $Ca_V3.1^{-/-}$ mice (70% ± 7% of baseline; $n = 7$, $P = 0.015$; Fig. 1 *C* and *D*). PPF was not significantly altered after LTD, again consistent with its postsynaptic site of expression (1.83 ± 0.15 vs. 1.78 ± 0.19, before and after induction protocol, respectively; $n = 7$, $P = 0.30$; Table S1). We conclude that T-type calcium channel activation is necessary for LTP but not LTD induction.

T-Type Channels Participate in the Firing Properties of the PC. The biophysical properties of low-voltage activated calcium channels allow them to be activated by subthreshold synaptic inputs and thus participate in synaptic integration and signaling. Indeed, we have previously shown that T-type channels are activated by synaptic activity at the PF–PC synapse (11, 22). Furthermore, they can contribute to the intrinsic firing behavior of neurons (23, 24). Here we have looked for their potential participation in the firing properties of PCs. In acute slices, where spontaneous excitatory synaptic inputs are severely reduced, we recorded PC activity (simple spikes) with extracellular electrodes. PCs of parasagittal slices of the vermis at 32 °C discharged at 36.2 ± 4.2 Hz with an interspike interval coefficient of variation (CV_{ISI}) 0.32 ± 0.04, CV_2 0.35 ± 0.05, $n = 23$; these data obtained in the presence of inhibition are consistent with previously reported data (25). TTA-P2 application resulted in a slight reduction in the firing frequency of 10.5% ± 2.2% ($n = 16$, $P < 0.001$), with no change in the CV_{ISI} (−1.5% ± 1%, $n = 16$; $P = 0.52$) or the CV_2 (+2.8% ± 2.8%, $n = 13$, $P = 0.45$) (Fig. 2 *A*–*C*). To account for a potential rundown, control values were measured at the same time points in the absence of TTA-P2; the firing frequency, CV_{ISI}, and CV_2 showed no change (0.0% ± 1.5% for frequency, 3.0% ± 3.5% for CV_{ISI}, and 0.8% ± 0.7% for CV_2; $n = 7$, P values > 0.15). Thus, T-type channel blockade only slightly reduces the simple spike frequency of PCs in vitro. However, disruption of PF–PC synaptic plasticity can also be associated with alterations in the regularity of PC spontaneous activity in

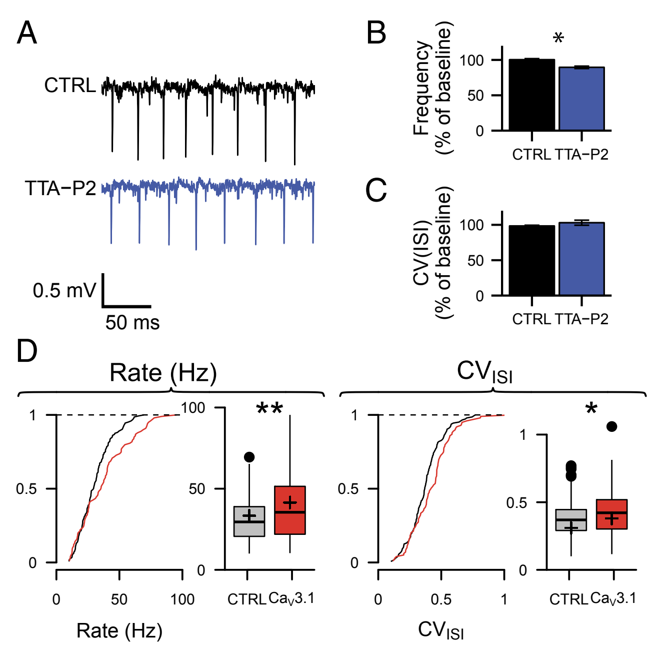

Fig. 2. Effects of T-type calcium channel functional inactivation on the spontaneous activity of PCs. (*A*–*C*) T-type calcium channel blockade slightly reduces the firing activity of PCs in vitro. (*A*) Representative traces from extracellular recordings of a PC before and after application of TTA-P2 in slices. (*B*) Normalized mean firing frequency and (*C*) coefficient of variation of the ISI in control and in TTA-P2 conditions. Paired experiments run on 16 cells and 13 cells, respectively. **P* < 0.05. (*D*) PC firing is altered in vivo. Cumulative distribution function and boxplot of the PCs' firing frequencies and CV_{ISI} (*Left* and *Right*, respectively). Boxplots represent minimum, first quartile, median, third quartile, and maximum values of the distribution. Filled circles represent outliers; the mean value is represented by a plus in the boxplot. Tests run on 99 and 144 cells recorded in control and $Ca_V3.1$ KO mice, respectively; statistical P values, **P* < 0.05, ***P* < 0.01.

vivo (1, 26), a situation where synaptic inputs are active and the temperature is physiological. Thus, we performed in vivo extracellular tetrode recordings of PCs in $Ca_V3.1^{-/-}$ and WT anesthetized mice (Fig. 2*D*). In contrast with the data obtained in slices, in vivo simple spike firing and irregularity were both increased in $Ca_V3.1^{-/-}$ mice (37.5 ± 2.0 Hz vs. 31.0 ± 1.1 Hz, P = 0.002; CV_{ISI} 0.39 ± 0.02 vs. 0.33 ± 0.02, P = 0.013; CV_2 0.42 ± 0.01 vs. 0.37 ± 0.01, P = 0.016, n = 99 cells in 6 $Ca_V3.1^{-/-}$ mice and n = 144 cells in 6 WT mice, pairwise t test). These data indicate that T-type calcium channel function extends beyond regulating simple changes in intrinsic excitability.

Effects of Genetic and Pharmacological Block of $Ca_V3.1$ Function on Basic Motor Performance and Motor Learning. Deletion of the $Ca_V3.1$ gene did not result in detectable morphological abnormalities (27, 28). KO mice did not display abnormal behavior in confined laboratory conditions: a 55-h activity survey did not indicate alteration of the global circadian activity (Fig. S1). Despite the changes in PC activity, $Ca_V3.1^{-/-}$ mice did not show obvious signs of motor performance deficits in the open field test, footprint analysis, or baseline optokinetic and vestibular eye movement tasks (Fig. S2). However, during more demanding motor coordination tasks such as walking on a small diameter elevated beam, performing an upside-down turn in the pole test or staying on a rotarod, $Ca_V3.1^{-/-}$ mice showed significant motor deficits. In the elevated beam test, both the time to achieve the test and the number of limb slips were significantly increased in $Ca_V3.1^{-/-}$ mice (P < 0.01, repeated measures ANOVA, in both cases) (Fig. 3*A*). In the pole test, time to turn (TT) was significantly longer in $Ca_V3.1^{-/-}$ mice (39 ± 11 s for $Ca_V3.1^{-/-}$ and 22 ± 7 s for WT, P < 0.001), together with a slight but not significantly higher fraction of animals that could not perform the task (Fig. 3*B*). In the rotarod test, time staying on the rod was always shorter for $Ca_V3.1^{-/-}$ mice, whether the protocol was done at constant speed or in acceleration (in all three cases, P < 0.001; repeated measures ANOVA) (Fig. 3*C*).

To address the issue of potential developmental deficits and/or compensation processes due to chronic absence of $Ca_V3.1$, we also analyzed the effect of acute TTA-P2 applications during the elevated beam task. TTA-P2, but not PBS, injections induced significant deficits on the elevated beam task in WT mice, whereas they had no significant impact on $Ca_V3.1^{-/-}$ mice (Fig. S3). WT mice treated with TTA-P2 and $Ca_V3.1^{-/-}$ mice treated with PBS showed also a different performance (P = 0.01), in line with the fact that TTA-P2 also blocks $Ca_V3.2$ and $Ca_V3.3$ subunits (21).

Cerebellar Learning Is Affected by Manipulation of $Ca_V3.1$ Function. To find out whether $Ca_V3.1$ in the cerebellum is indeed specifically involved in the motor coordination deficits, we next investigated adaptation of the VOR. This task is known to be controlled by the vestibulocerebellum (1, 3). When the mice were subjected to a short-term gain-decrease paradigm (i.e., in phase 5° optokinetic and vestibular stimulation at 0.6 Hz during 5 × 10 min training sessions), the gain during VOR in the dark decreased to 56% ± 4% in WT mice (Fig. 4). This VOR gain-decrease paradigm was significantly impaired by pharmacological block with TTA-P2 (P = 0.010; repeated measures ANOVA), but it was not significantly affected in $Ca_V3.1$ mice (P = 0.95; repeated measures ANOVA), possibly reflecting developmental compensation (Fig. 4). Instead, when we used the more demanding and sensitive, long-term VOR phase-reversal training paradigm (i.e., 4 consecutive days of in-phase stimulation at 0.6 Hz during which the amplitude of the optokinetic stimulus increased up to 10°, while the vestibular stimulus was maintained at 5°), both WT mice injected with TTA-P2 and $Ca_V3.1$ mice showed significant impairment compared with control data (Fig. 4). TTA-P2 injections affected phase reversal significantly on days 2, 3, and 4 (P = 0.044, 0.0001, and 0.0001, respectively; repeated measures ANOVA), and the $Ca_V3.1^{-/-}$ mice showed significant deficits on days 3 and 4 (both P < 0.002; repeated measures ANOVA). After each day of training, mice were placed in the dark until the next day, when their VOR was recorded again. Consolidation of learning, calculated from the response of the next day, did not differ between controls, $Ca_V3.1^{-/-}$ mice, and mice injected with TTA-P2 (for all comparisons, P > 0.45; one-way ANOVA) (for the first days of comparison, see Fig. 4).

Discussion

In this study, we reveal a role of the T-type calcium channels in cerebellar plasticity and learning. Activation of T-type calcium channels turned out to be necessary for the induction of postsynaptic LTP but not LTD at PF–PC synapses and to contribute to the firing properties of the PC. These functions may explain the deficits observed in demanding cerebellar motor performance and motor learning tasks following both genetic and acute pharmacological inactivation of T-type channels.

$Ca_V3.1$ Functional Inactivation Results in Specific Deficits in PF–PC Synaptic Plasticity. Even though PC spines are largely devoid of Ca-permeable AMPA and NMDA receptors (4, 5), calcium signaling can be locally ensured by release from intracellular

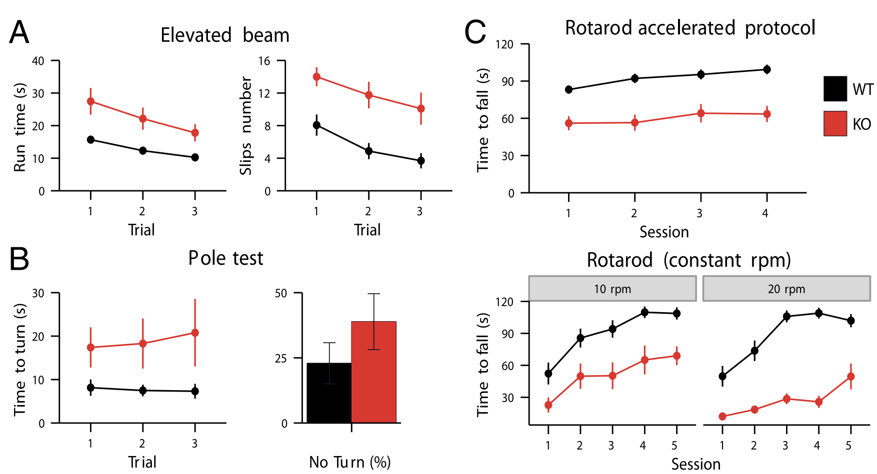

Fig. 3. Motor behavioral deficit after inactivation of T-type channels. Coordination was significantly impaired in $Ca_V3.1^{-/-}$ mice (*A*–*C*) comparison of motor performance of WT and $Ca_V3.1^{-/-}$ mice (black and red symbols, respectively, and n = 16 and 12). For details on the individual tests, see *Methods*. (*A*) Motor impairment in the elevated beam test. Mice were made to walk on a horizontal beam. Time to perform on a 100-cm-long run was measured as well as the number of times hindlimbs slipped off the beam during three trials. $Ca_V3.1^{-/-}$ mice take more time to achieve the test (P < 0.01, repeated measures ANOVA) (*A*, *Left*) and stumbled more often than WT animals (the rear leg slips off the bar) (P < 0.01, repeated measures ANOVA) (*A*, *Right*)). Mice performance increased during the three trials for both the run time and the number of slips, $F(2, 52)$ > 20, P < 0.001, for both phenotypes. (*B*) Motor impairment in the pole test. The animal was positioned with head up close to the pole top. It had to turn before going head down the rod to return to its cage. TT measured the delay until the mouse was head down. Mutant animals took longer time to reach the box (TT = 39 ± 11 s for $Ca_V3.1^{-/-}$ and 22 ± 7 s for WT, P < 0.001) (*B*, *Left*). There is a slight but nonsignificant increase of $Ca_V3.1^{-/-}$ mice that could not achieve the task (*B*, *Right*). (*C*) Motor impairment in the rotarod test. The time $Ca_V3.1^{-/-}$ mice stayed on the rod with a constant rotation speed (10 rpm or 20 rpm) or with accelerating speed (from 4 to 40 rpm in 2 min) was significantly shorter for $Ca_V3.1^{-/-}$ (10 rpm, P < 0 0.001; 20 rpm, P < 0 0.001; accelerated protocol, P < 0.001; repeated measures ANOVA).

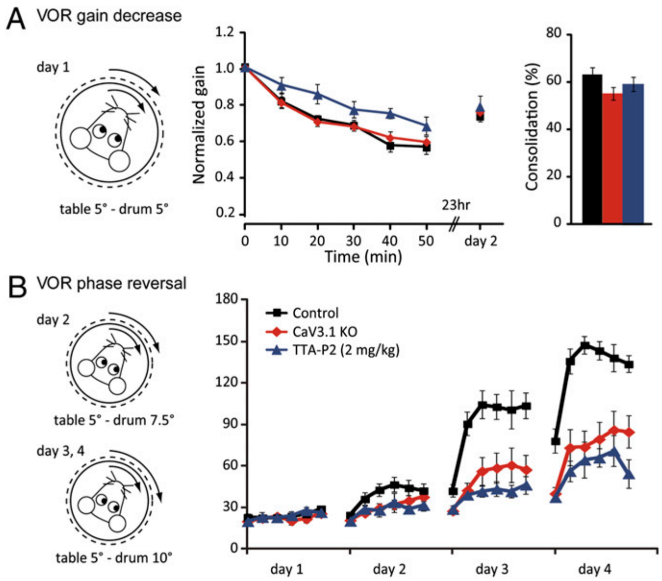

Fig. 4. Cerebellar learning is affected by manipulation of $Ca_V3.1$ function. Short- (*A*) and long-term adaptation (*B*) of the VOR gain was induced by mismatched vestibular and visual stimulation. (*A*) Five 10-min sessions of in-phase drum and table stimulation resulted in a decrease of VOR gain to 56% ± 4% of baseline value ($n = 8$). A similar decrease was seen in $Ca_V3.1$ KO mice (59% ± 3%, $n = 12$, $P = 0.95$ for the curve, repeated measures ANOVA), but not in mice injected with TTA-P2 (67% ± 7%, $n = 7$, $P = 0.010$ for the curve, repeated measures ANOVA). Consolidation of VOR gain decrease was found not to be different between groups ($P = 0.75$, one-way ANOVA). (*B*) Next, mice were subjected to 3 additional days with increasing amplitude of visual stimulation during the training sessions, aimed at reversing VOR phase. This highly demanding task revealed significant deficits in cerebellar learning in $Ca_V3.1$ KO mice (days 3 and 4, $P < 0.002$, repeated measures ANOVA) and in mice injected with TTA-P2 (day 2, $P = 0.044$; days 3 and 4, $P < 0.0001$, repeated measures ANOVA).

stores after mGluR1 activation (18, 29–31) after opening of non-selective cation channels (32–34), the transient receptor potential channel 3 (TRPC3) possibly being one of those (35). In addition, high- and low-voltage activated calcium channels are present in PCs. We have recently shown that T-type calcium channels contribute to the PF–PC synaptic events, bringing a noticeable Ca^{2+} entry into the postsynaptic spine (11, 22). By inactivating T-type channel function following genetic deletion of the $Ca_V3.1$ subunit or acute application of an antagonist, we show here that they also contribute to the induction of LTP. LTP develops in response to repetitive stimulation of PF fibers and is known to depend on postsynaptic calcium signaling, suggesting that T-type channels provide at least part of the Ca^{2+} entry necessary for LTP induction. Noticeably, we have used a physiological concentration of divalent ions (see also refs. 36 and 37 for Ca^{2+} and Mg^{2+} concentrations, respectively), thereby limiting the depolarization of the spiny branchlets. This stimulus protocol may be better in line with the sparse PF inputs that probably occur under more physiological circumstances and may avoid the spurious P/Q channel activation by strong PF bundle stimulation. LTD is induced by conjunctive stimulation of PFs and CFs (16, 17, 19) and depends on the activation of mGluR1 receptors and IP_3 receptors. We show that functional inactivation of T-type channels does not affect LTD. This is consistent with its known dependency on high postsynaptic calcium levels (15–17, 38) (see also reviews in refs. 39, 40), presumably resulting from the activation of P/Q calcium channels after the strong depolarization ensuing CF activity plus release from internal stores (31, 41).

PC Firing Properties. T-type channels can affect PC firing in two ways. First, as a depolarizing conductance presenting a non-negligible window current, they can depolarize the somatic compartment and eventually the axon initial segment and thereby increase the spontaneous firing rate (42). Consistent with this, we show here that T-type channel blockade slightly reduces the spontaneous firing activity in vitro. The situation, however, is different in vivo, where synaptic inputs are active and where temperature is more physiological. Under these conditions, T-type channels in spines may participate in the determination of PC firing pattern as part of the synaptic conductance. Indeed, we have observed an increased and more irregular firing rate in PCs of $Ca_V3.1$ KO mice in vivo, supporting the idea of a key role played by spine T-type channels under physiological conditions. However, we cannot exclude a role for $Ca_V3.1$ channels in other cells of the olivo-cerebellar circuit.

Plasticity and Motor Learning. Since the seminal work of Ito (16, 43), learning processes in the cerebellum have been linked to a reduction in the weight of the PF–PC synapse. In line with this, blocking LTD has been expected to impair motor learning. Indeed, LTD is absent in a number of cerebellar mutants displaying motor impairment (44–46). However, this assertion has been recently questioned (47), and LTP has been proposed as a key process involved in cerebellar learning (1, 3, 26). Indeed, one can observe increased cutaneous receptive fields of PCs after repetitive stimulation of PFs via peripheral afferents (48). This view is also supported by our observation of concomitant impaired LTP and motor learning, with no alteration of LTD.

The $Ca_V3.1$ KO mouse is not ataxic, as can occur, for example, after alteration of IP3R-mediated Ca^{2+} release (31, 49) or after mutations of P/Q-type calcium channels (50–52), both of which probably affect the PC physiology more severely and/or have developmental issues. T-type channels play a more subtle role in the control of motor coordination. Deletion of T-type channels impairs demanding motor behaviors, such as staying on a small-diameter rotarod, walking on a thin elevated beam, or turning at the top of a pole, all of which involve a cerebellar component. Moreover, after inactivation of T-type channels, VOR learning is impaired but not fully abolished, as seen after protein phosphatase 2B (PP2B) deletion (1, 47, 53). The reason why L7-PP2B mutant mice have a more severe phenotype than $Ca_V3.1$ KO may eventually be linked to the additional role of PP2B in intrinsic plasticity (1). Disruption of overall gain reset by intrinsic plasticity impairment in L7-PP2B mice may deteriorate basal cerebellar function (3). Our data also indicate that the observed motor learning phenotype does not arise from broad defects in motor function. Indeed, basal vestibular and optokinetic reflexes remain normal. In addition, mice behave in a similar way during the open field test and have the same nycthemeral activity during a 55-h survey. Finally, even though other subunits ($Ca_V3.2$ and $Ca_V3.3$) also form T-type channels, $Ca_V3.1$ genetic inactivation largely reproduces the cerebellar phenotype observed upon acute application of TTA-P2. This similarity suggests that compensatory effects by iso-proteins are limited in our $Ca_V3.1$ mutant mice. Thus, our data support the idea of an essential role of $Ca_V3.1$ in cerebellar motor learning. Whether this is due exclusively to the absence of $Ca_V3.1$ channels in PCs or to effects distributed over the olivocerebellar circuit will need further investigation.

In conclusion, our data indicate that $Ca_V3.1$ T-type channels contribute to LTP at the PF to PC synapse and thereby to related changes in firing rate dynamics and performance in demanding cerebellar learning tasks. This reveals a specific role of postsynaptic voltage-dependent T-type calcium channel in the induction of plasticity and learning. We propose that the recruitment modalities of $Ca_V3.1$ T-type channels as well as their modulation contribute to the definition of specific synaptic plasticity rules in the cerebellar cortex, highlighting their impact on learning.

Methods

All electrophysiological and behavioral experiments were conducted in compliance with French and European laws and policies. Mouse eye movement

NEUROSCIENCE

experiments were performed in accordance with The Dutch Ethical Committee (DEC) for animal experiments.

Animals. Mice lacking the cacna1g gene (encoding $Ca_V3.1$) were produced as previously described (28).

T-Type Channel Antagonist, TTA-P2. TTA-P2 [(3,5-dichloro-*N*-[1-(2,2-dimethyl-tetrahydro-pyran-4-ylmethyl)-4-fluoropiperidin-4-ylmethyl]-benzamide), Merck, com-pound (S)-5] (21) was made up as a 10 mM stock solution in dimethyl sulfoxide (DMSO); aliquots were kept at –20 °C and diluted for use as indicated at 1 μM concentrations known to block T-type calcium channels (21, 23).

LTP/LTD Experimental Protocols. Transverse cerebellar slices (300 μm thick) of 45–75-d-old C57BL/6 mice were prepared with 50 μM (2R)-amino-5-phosphonovaleric acid (D-APV) (Abcam) added to the slicing solution to protect the tissue. Slices were visualized using a 40× water-immersion objective and infrared optics. The recording chamber was continuously perfused at a rate of 3 mL/min with a solution containing (mM) 125 NaCl, 2.5 KCl, 1.5 $CaCl_2$, 1.8 $MgCl_2$, 1.25 NaH_2PO_4, 26 $NaHCO_3$, 25 glucose, and 10 tricine, a Zn^{2+} ion buffer (54, 55), and 20 μM bicuculline methochloride (Tocris) bubbled with 95% (vol/vol) O_2/5% CO_2 (pH 7.4).

Patch pipettes had 2.0–4.0 MΩ resistances with an internal solution that contained (in mM) 120 KGluconate, 0.5 K_3Citrate, 0.5 L(–)Malic acid, 0.008 Oxaloacetic acid, 0.18 α-Ketoglutaric acid, 0.2 Pyridoxal 5′-phosphate, 5 L-Alanine, 0.15 Pyruvic acid, 15 L- Glutamine, 4 L-Asparagine, 1 L-Glutathione reduced, 0.5 NAD^+, 5 Phosphocreatine K_2, 10 Hepes, 0.1 K_3EGTA, 4 KCl, 2.2 K_2Phosphate, 3.5 NaAcetate, 0.05 $CaCl_2$, 2.1 Mg-ATP, 0.4 Na-GTP, 1.4 Na-ATP, pH adjusted to 7.3 with KOH. Unless otherwise stated, cells were voltage-clamped at −70 mV in the whole-cell configuration. Series resistance was held between 4 and 10 MΩ and compensated with settings of 90% in an Axopatch 700B amplifier. Whole-cell recordings were filtered at 2 kHz and digitized at 10 kHz. Long-term potentiation was induced by stimulating the PF beam with five pulses at 200 Hz every second for 5 min. Long-term depression was induced by stimulating PFs (two pulses at 200 Hz) followed by CF stimulation (four pulses at 400 Hz) 100 ms later every second for 5 min. During LTP induction, PCs were held in current clamp at −70 mV. LTP and LTD were quantified as the ratio between EPSC charge after induction (mean of 15 sweeps between 30 and 35 min after induction) and control EPSC charge (mean of 15 sweeps immediately before induction). Experiments were performed at 32 °C. To evoke PF EPSCs, a 8–12 μm tip diameter glass pipette filled with Hepes-buffered saline was positioned on the molecular layer surface to stimulate PFs at 100–500 μm from the recorded PC. Images were taken every 5 min, and experiments showing significant slice movement were discarded. Stimulation intensity was fixed at the beginning of the experiment between 1 and 15 V for 50–200 μs. At 0.05 Hz, pairs of test pulses at an interval of 50 ms were applied, enabling the paired-pulse ratio to be monitored. Recordings were made in lobules 3–8 of the vermis cortex. To stimulate CF during LTD induction, a glass pipette filled with Hepes-buffered saline was positioned on the granular layer in the vicinity of the recorded PC. Stimulation intensity was fixed between 1 and 15 V for a duration between 50 and 200 μs. PClamp 10.3 software (Molecular Dynamics) was used for data acquisition, and analysis was done with in-house software (Python). Data were statistically analyzed using Mann–Whitney *U* test.

Extracellular Recordings. Parasagittal cerebellar slices (300 μm thick) of at least 2-mo-old C57BL/6 mice were prepared as above. The recording chamber was continuously perfused at a rate of 3 mL/min with a solution containing (mM) 125 NaCl, 3.5 KCl, 2 $CaCl_2$, 1 $MgCl_2$, 1.25 NaH_2PO_4, 26 $NaHCO_3$, 25 glucose bubbled with 95% O_2/5% CO_2 (pH 7.4). No $GABA_A$ antagonists were added to the bath solution. Recording pipettes had 3.0–4.0 MΩ resistances with an internal solution that contained (in mM) 141 NaCl, 2.5 KCl, 1.25 NaH_2PO_4, 10 Hepes, 2 $CaCl_2$, 1 $MgCl_2$ with pH adjusted at 7.4 (NaOH). Firing pattern was characterized by both CV_{ISI} and CV_2. CV_2 was measured with $CV_2 = 2\,|ISI_{n+1} - ISI_n|/(ISI_{n+1} + ISI_n)$. Data were statistically analyzed using two-sided Mann–Whitney *U* test.

In Vivo Electrophysiology. The surgery was carried out as described in refs. 56, 57 on male C57BL/6 mice using urethane for animal anesthesia. The skull was opened at −6.72 AP (anteroposterior) and 0 ML (mediolateral), or −6.36 AP and 1.5 ML stereotaxic coordinates and meninges were removed to insert the electrodes. Simultaneous multiple single-unit recordings from the PC layer (as determined by the presence of complex spikes) were obtained using commercial tetrodes (Thomas Recording, tungsten electrodes in a quartz matrix) at 0.5 to ∼3.5 mm depth in the vermis. Wire tips were gold-plated (gold solution, Sifco) to reduce their impedance (200–300 kΩ). The tetrode was advanced in small increments of 10–50 μm. Cerebellar cortex layers could be discriminated: the PC layer displayed an intense cellular activity and distinctive complex spikes, whereas in the proximal molecular layer complex spikes appeared as 1–3 ms monophasic waves.

To isolate spikes, continuous wide-band extracellular recordings were first filtered off-line with a two-pole Butterworth 500 Hz high-pass filter. Spikes were extracted by thresholding the filtered trace and the main parameters of their waveform extracted (width and amplitude on the four channels). The data were hand clustered by polygon-cutting in 2-dimensional projections of the parameter space using Xclust (M. Wilson, Massachusetts Institute of Technology, Cambridge, MA). The quality of clustering was evaluated by inspecting the autocorrelograms of the units. The stationarity of unit activity was monitored by calculating the average rate each second over the recording period. Further analysis was performed with GNU R (58). Data were statistically analyzed using pairwise *t* test.

Behavioral Analysis. After a 2 wk adaptation, characteristics of global locomotor activity were first assessed by direct observation of the animals' exploration in an activity chamber (45 × 45 × 30 cm) during 10 min using ANYmaze video-tracking system (Stoelting).

To analyze footprints, mice were allowed to walk on a 0.5-m-long band of blotting paper after their paws had been colored with distinct color inks for anterior and posterior paws.

The rotarod (L2 8200, Bioseb) was adapted for mice. It had a central rod of 3 cm diameter, and the 5-cm-wide running belts were separated by 15-cm-diameter circular partitions. Time to fall was measured with different accelerations.

The rod (9 mm diameter) used for the walk on an elevated beam rested at one end on a platform giving access to the animal cage. For a trial this platform was positioned successively at 5, 15, and 50 cm, and finally time to perform a 100 cm run was measured as well as the number of times any limb slipped (three trials).

In the pole test (59), a vertical rod (8 mm diameter and 50 cm long, covered with tape) was placed in the animal cage. The animal was positioned with the head up close to the pole top and had to turn before going head down the rod to return to its cage. TT—to be head down—and total time (TT + descent time)—to be back to cage—were measured. If a mouse did not turn around and went down head up, the same duration was attributed to the TT and descent time. Maximum duration was fixed at 120 s (five trials in a day at 5-min intervals). Data were statistically analyzed using a repeated-measures ANOVA followed by Tukey post hoc comparisons to determine significance levels, unless otherwise stated.

Eye-Movement Recordings. Mice were prepared for multiple days of awake, head-restrained recordings of compensatory eye movements (51). Briefly, under general anesthesia with isoflurane (∼1.5% and O_2), a pedestal was fixed to the frontal and parietal parts of the skull. The pedestal consisted of a U-shaped holder (6 × 4 mm at base) with a magnet (4 × 4 × 2 mm) and a screw hole. After an at least 3 d recovery, mice were connected to a bar (equipped with a similar magnet); the connection was fixed with a screw, and the body of the mouse was restrained in a custommade plastic tube. The immobilized mouse was fixed onto a turntable (diameter 60 cm), surrounded by a cylindrical screen (diameter 63 cm) with a random-dotted pattern. Two table-fixed infrared emitters (maximum output, 1 W; dispersion angle, 7°; peak wavelength, 880 nm) illuminated the eye during the recording, and a third emitter was connected to the camera and aligned horizontally with the camera's optical axis, to produce the corneal reflection (CR). Optokinetic and vestibulo-ocular reflexes (in light and dark) were elicited by rotating the screen and turntable, respectively, at different frequencies (AC servo-motors, Harmonic Drive AG). Table and drum positions were recorded by potentiometers, and the signal was digitized (CED Limited) and stored for off-line analysis. Eye movements, relative to the CR, were recorded at 240 Hz using eye-tracking software (ETL-200, ISCAN systems). Calibrations were performed as described previously (51). Gain and phase values of the eye movements were calculated using a custommade Matlab routine (MathWorks Inc.). Briefly, the eye and stimulus traces were differentiated, low-pass filtered (to remove fast phases), averaged over the recorded cycles, and fitted. Gains were calculated as the amplitude of the fitted eye velocity signal, divided by stimulus velocity, and phase as the temporal difference between fits in degrees. Consolidation percentage was calculated as 100*(td2max–t0)/(td1min–t0), where t0 stands for value at the start of day 1, td1min for lowest value during 50 min training on day 1, and td2 as the highest value on day 2. Consolidation data were statistically analyzed using one-way ANOVA, all other data using a repeated-measures

ANOVA, both followed by Tukey post hoc comparisons to determine significance levels.

ACKNOWLEDGMENTS. We acknowledge the contribution of Dr. M. Kano and Dr. K. Sakimura, who provided us with the $Ca_V3.1$ KO mice. We also thank Boris Barbour for comments on the manuscript. TTA-P2 was provided by Merck and Co., Inc. R.L. was successively supported by a 3-year Centre National de la Recherche Scientifique (CNRS) doctoral fellowship and a 1-year Fondation pour la Recherche Médicale (FRM)/Université Pierre et Marie Curie fellowship, and G.B. was funded by Région Ile de France. The project was funded by CNRS and Ecole Normale Supérieure (to A.F.), ANR-08-SYSC-005 (to Boris Barbour), ANR-09-MNPS-38 and ANR-11-BSV4-028 (to C.L.), ANR-BLAN-SVSE4-LS-120230-DC/MM/ and FRM DEQ20120323730 (to L.R.-R.), Dutch Organization for Medical Sciences (C.I.D.Z.), Life Sciences (to M.S. and C.I.D.Z.), Erasmus University Rotterdam Fellowship (to M.S.), Center Neuro-Basic (C.I.D.Z.), and European Research Council Advanced grant (C.I.D.Z.).

1. Schonewille M, et al. (2010) Purkinje cell-specific knockout of the protein phosphatase PP2B impairs potentiation and cerebellar motor learning. *Neuron* 67(4):618–628.
2. Boyden ES, Raymond JL (2003) Active reversal of motor memories reveals rules governing memory encoding. *Neuron* 39(6):1031–1042.
3. Gao Z, van Beugen BJ, De Zeeuw CI (2012) Distributed synergistic plasticity and cerebellar learning. *Nat Rev Neurosci* 13(9):619–635.
4. Rosenmund C, Legendre P, Westbrook GL (1992) Expression of NMDA channels on cerebellar Purkinje cells acutely dissociated from newborn rats. *J Neurophysiol* 68(5): 1901–1905.
5. Häusser M, Roth A (1997) Dendritic and somatic glutamate receptor channels in rat cerebellar Purkinje cells. *J Physiol* 501(Pt 1):77–95.
6. Llinás R, Sugimori M (1980) Electrophysiological properties of in vitro Purkinje cell dendrites in mammalian cerebellar slices. *J Physiol* 305:197–213.
7. Westenbroek RE, et al. (1995) Immunochemical identification and subcellular distribution of the alpha 1A subunits of brain calcium channels. *J Neurosci* 15(10): 6403–6418.
8. Indriati DW, et al. (2013) Quantitative localization of $Ca_v2.1$ (P/Q-type) voltage-dependent calcium channels in Purkinje cells: Somatodendritic gradient and distinct somatic coclustering with calcium-activated potassium channels. *J Neurosci* 33(8): 3668–3678.
9. Talley EM, et al. (1999) Differential distribution of three members of a gene family encoding low voltage-activated (T-type) calcium channels. *J Neurosci* 19(6): 1895–1911.
10. Isope P, Murphy TH (2005) Low threshold calcium currents in rat cerebellar Purkinje cell dendritic spines are mediated by T-type calcium channels. *J Physiol* 562(Pt 1): 257–269.
11. Hildebrand ME, et al. (2009) Functional coupling between mGluR1 and Cav3.1 T-type calcium channels contributes to parallel fiber-induced fast calcium signaling within Purkinje cell dendritic spines. *J Neurosci* 29(31):9668–9682.
12. Jörntell H, Ekerot CF (2006) Properties of somatosensory synaptic integration in cerebellar granule cells in vivo. *J Neurosci* 26(45):11786–11797.
13. Chadderton P, Margrie TW, Häusser M (2004) Integration of quanta in cerebellar granule cells during sensory processing. *Nature* 428(6985):856–860.
14. van Beugen BJ, Gao Z, Boele HJ, Hoebeek F, De Zeeuw CI (2013) High frequency burst firing of granule cells ensures transmision at the parallel fiber to Purkinje cell synapse at the cost of temporal coding. *Front Neural Circuits* 7:95.
15. Coesmans M, Weber JT, De Zeeuw CI, Hansel C (2004) Bidirectional parallel fiber plasticity in the cerebellum under climbing fiber control. *Neuron* 44(4):691–700.
16. Ito M, Sakurai M, Tongroach P (1982) Climbing fibre induced depression of both mossy fibre responsiveness and glutamate sensitivity of cerebellar Purkinje cells. *J Physiol* 324:113–134.
17. Sakurai M (1987) Synaptic modification of parallel fibre-Purkinje cell transmission in in vitro guinea-pig cerebellar slices. *J Physiol* 394:463–480.
18. Finch EA, Augustine GJ (1998) Local calcium signalling by inositol-1,4,5-trisphosphate in Purkinje cell dendrites. *Nature* 396(6713):753–756.
19. Wang SS, Denk W, Häusser M (2000) Coincidence detection in single dendritic spines mediated by calcium release. *Nat Neurosci* 3(12):1266–1273.
20. Lev-Ram V, Wong ST, Storm DR, Tsien RY (2002) A new form of cerebellar long-term potentiation is postsynaptic and depends on nitric oxide but not cAMP. *Proc Natl Acad Sci USA* 99(12):8389–8393.
21. Shipe WD, et al. (2008) Design, synthesis, and evaluation of a novel 4-aminomethyl-4-fluoropiperidine as a T-type Ca2+ channel antagonist. *J Med Chem* 51(13):3692–3695.
22. Ly R, et al. (2012) Electrical contribution of postsynaptic T-type calcium channels to parallel fiber-Purkinje cell synaptic transmission. *2012 Neuroscience Meeting Planner* (Society for Neuroscience, New Orleans, LA). Program No. 477.05.
23. Dreyfus FM, et al. (2010) Selective T-type calcium channel block in thalamic neurons reveals channel redundancy and physiological impact of I(T)window. *J Neurosci* 30(1): 99–109.
24. Bender KJ, Trussell LO (2009) Axon initial segment Ca2+ channels influence action potential generation and timing. *Neuron* 61(2):259–271.
25. Häusser M, Clark BA (1997) Tonic synaptic inhibition modulates neuronal output pattern and spatiotemporal synaptic integration. *Neuron* 19(3):665–678.
26. De Zeeuw CI, et al. (2011) Spatiotemporal firing patterns in the cerebellum. *Nat Rev Neurosci* 12(6):327–344.
27. Kim D, et al. (2001) Lack of the burst firing of thalamocortical relay neurons and resistance to absence seizures in mice lacking alpha(1G) T-type Ca(2+) channels. *Neuron* 31(1):35–45.
28. Petrenko AB, Tsujita M, Kohno T, Sakimura K, Baba H (2007) Mutation of alpha1G T-type calcium channels in mice does not change anesthetic requirements for loss of the righting reflex and minimum alveolar concentration but delays the onset of anesthetic induction. *Anesthesiology* 106(6):1177–1185.
29. Canepari M, Ogden D (2006) Kinetic, pharmacological and activity-dependent separation of two Ca2+ signalling pathways mediated by type 1 metabotropic glutamate receptors in rat Purkinje neurones. *J Physiol* 573(Pt 1):65–82.
30. Takechi H, Eilers J, Konnerth A (1998) A new class of synaptic response involving calcium release in dendritic spines. *Nature* 396(6713):757–760.
31. Miyata M, et al. (2000) Local calcium release in dendritic spines required for long-term synaptic depression. *Neuron* 28(1):233–244.
32. Hirono M, Konishi S, Yoshioka T (1998) Phospholipase C-independent group I metabotropic glutamate receptor-mediated inward current in mouse purkinje cells. *Biochem Biophys Res Commun* 251(3):753–758.
33. Canepari M, Papageorgiou G, Corrie JE, Watkins C, Ogden D (2001) The conductance underlying the parallel fibre slow EPSP in rat cerebellar Purkinje neurones studied with photolytic release of L-glutamate. *J Physiol* 533(Pt 3):765–772.
34. Tempia F, Alojado ME, Strata P, Knöpfel T (2001) Characterization of the mGluR(1)-mediated electrical and calcium signaling in Purkinje cells of mouse cerebellar slices. *J Neurophysiol* 86(3):1389–1397.
35. Hartmann J, et al. (2008) TRPC3 channels are required for synaptic transmission and motor coordination. *Neuron* 59(3):392–398.
36. Silver IA, Erecińska M (1990) Intracellular and extracellular changes of [Ca2+] in hypoxia and ischemia in rat brain in vivo. *J Gen Physiol* 95(5):837–866.
37. Chutkow JG, Meyers S (1968) Chemical changes in the cerebrospinal fluid and brain in magnesium deficiency. *Neurology* 18(10):963–974.
38. Lev-Ram V, Makings LR, Keitz PF, Kao JP, Tsien RY (1995) Long-term depression in cerebellar Purkinje neurons results from coincidence of nitric oxide and depolarization-induced Ca2+ transients. *Neuron* 15(2):407–415.
39. Jörntell H, Hansel C (2006) Synaptic memories upside down: Bidirectional plasticity at cerebellar parallel fiber-Purkinje cell synapses. *Neuron* 52(2):227–238.
40. Finch EA, Tanaka K, Augustine GJ (2012) Calcium as a trigger for cerebellar long-term synaptic depression. *Cerebellum* 11(3):706–717.
41. Daniel H, et al. (1999) Inositol-1,4,5-trisphosphate-mediated rescue of cerebellar long-term depression in subtype 1 metabotropic glutamate receptor mutant mouse. *Neuroscience* 92(1):1–6.
42. Raman IM, Bean BP (1999) Ionic currents underlying spontaneous action potentials in isolated cerebellar Purkinje neurons. *J Neurosci* 19(5):1663–1674.
43. Ito M, Kano M (1982) Long-lasting depression of parallel fiber-Purkinje cell transmission induced by conjunctive stimulation of parallel fibers and climbing fibers in the cerebellar cortex. *Neurosci Lett* 33(3):253–258.
44. Ichise T, et al. (2000) mGluR1 in cerebellar Purkinje cells essential for long-term depression, synapse elimination, and motor coordination. *Science* 288(5472):1832–1835.
45. Goossens J, et al. (2001) Expression of protein kinase C inhibitor blocks cerebellar long-term depression without affecting Purkinje cell excitability in alert mice. *J Neurosci* 21(15):5813–5823.
46. Miyata M, Okada D, Hashimoto K, Kano M, Ito M (1999) Corticotropin-releasing factor plays a permissive role in cerebellar long-term depression. *Neuron* 22(4): 763–775.
47. Schonewille M, et al. (2011) Reevaluating the role of LTD in cerebellar motor learning. *Neuron* 70(1):43–50.
48. Jörntell H, Ekerot CF (2003) Receptive field plasticity profoundly alters the cutaneous parallel fiber synaptic input to cerebellar interneurons in vivo. *J Neurosci* 23(29): 9620–9631.
49. Wagner W, Brenowitz SD, Hammer JA, 3rd (2011) Myosin-Va transports the endoplasmic reticulum into the dendritic spines of Purkinje neurons. *Nat Cell Biol* 13(1): 40–48.
50. Fletcher CF, et al. (2001) Dystonia and cerebellar atrophy in Cacna1a null mice lacking P/Q calcium channel activity. *FASEB J* 15(7):1288–1290.
51. Hoebeek FE, et al. (2005) Increased noise level of purkinje cell activities minimizes impact of their modulation during sensorimotor control. *Neuron* 45(6):953–965.
52. Todorov B, et al. (2012) Purkinje cell-specific ablation of Cav2.1 channels is sufficient to cause cerebellar ataxia in mice. *Cerebellum* 11(1):246–258.
53. De Zeeuw CI, et al. (1998) Expression of a protein kinase C inhibitor in Purkinje cells blocks cerebellar LTD and adaptation of the vestibulo-ocular reflex. *Neuron* 20(3): 495–508.
54. Paoletti P, Ascher P, Neyton J (1997) High-affinity zinc inhibition of NMDA NR1-NR2A receptors. *J Neurosci* 17(15):5711–5725.
55. Bidoret C, Ayon A, Barbour B, Casado M (2009) Presynaptic NR2A-containing NMDA receptors implement a high-pass filter synaptic plasticity rule. *Proc Natl Acad Sci USA* 106(33):14126–14131.
56. de Solages C, et al. (2008) High-frequency organization and synchrony of activity in the purkinje cell layer of the cerebellum. *Neuron* 58(5):775–788.
57. Gao H, Solages Cd, Lena C (2012) Tetrode recordings in the cerebellar cortex. *J Physiol Paris* 106(3-4):128–136.
58. R Development Core Team (2004) *R: A Language and Environment for Statistical Computing* (R Foundation for Statistical Computing, Vienna, Austria).
59. Bouët V, et al. (2007) Sensorimotor and cognitive deficits after transient middle cerebral artery occlusion in the mouse. *Exp Neurol* 203(2):555–567.